

Incorporation of *Paramecium* axonemal tubulin into higher plant cells reveals functional sites of microtubule assembly

(mitosis/plant microtubule organizing centers/copolymerization/phragmoplast/nuclear envelope)

MARYLIN VANTARD*^{†‡}, NICOLETTE LEVILLIERS[§], ANNE-MARIE HILL[§], ANDRÉ ADOUTTE[§],
AND ANNE-MARIE LAMBERT*[†]

*Laboratoire de Biologie Cellulaire Végétale, Unité Associée 1182 du Centre National de la Recherche Scientifique, Université Louis Pasteur, 28 rue Goethe, 67083 Strasbourg Cedex, France; and [§]Laboratoire de Biologie Cellulaire 4, Unité Associée 1134 du Centre National de la Recherche Scientifique, Université Paris-Sud, 91405 Orsay Cedex, France

Communicated by Lynn Margulis, June 22, 1990 (received for review March 6, 1990)

ABSTRACT Incorporation of *Paramecium* axonemal tubulin into lysed endosperm cells of the higher plant *Haemanthus* enabled us to identify sites of microtubule assembly. This exogenous *Paramecium* tubulin could be traced by specific antibodies that do not stain endogenous plant microtubules. Intracellular copolymerization of protozoan and higher plant tubulins gave rise to hybrid polymers that were visualized by immunofluorescence and by immunoelectron microscopy. The addition of exogenous tubulin revealed many free ends of endogenous microtubules that were competent to assemble ciliate tubulin. The functional roles of the nuclear surface and the equatorial region of the phragmoplast as plant microtubule-organizing centers, which were revealed by the intense incorporation of exogenous tubulin, are discussed. These data shed light on the present debate on higher plant microtubule organizing centers.

Temporal and spatial regulation of microtubule (MT) assembly in acentriolar higher plant cells remains poorly understood, because of the lack of data from a functional assay of nucleation capacity that would unambiguously identify plant microtubule-organizing centers (MTOCs). Indirect information has been obtained through immunocytochemical and ultrastructural approaches. Human autoantibodies that stain pericentriolar nucleating material in animal cells (1, 2) decorate the periphery of the nucleus and the spindle poles of higher plant cells (3, 4). However, the significance of this cross-reactivity has been questioned (5). It has also been suggested that sites of MT anchoring, detected by anti-tubulin labeling (6–8), may correspond to nucleation centers since electron dense material resembling pericentriolar material is usually associated with them (9–12). Our specific aims were to obtain functional evidence that the nuclear envelope in higher plants acts as a MT nucleation center and to study the origin of phragmoplast MT assembly during anaphase–telophase.

For this purpose we used a method that is derived from the analysis of MT dynamics and nucleation sites in animal cells in which a “reporter” tubulin is microinjected. The reporter tubulin can either be labeled tubulin (13, 14) or tubulin from a distant organism for which a species-specific anti-tubulin antibody is available (15, 16). In this context, we have developed an *in vitro* system of lysed *Haemanthus* endosperm cells (17) in which unmodified *Paramecium* axonemal (PA) tubulin is incorporated and then selectively labeled by its homologous antibody (15, 18, 19). *Haemanthus* endosperm cells are remarkably suited for investigating plant mitosis and cytoskeleton (6–8, 20), and their lack of cell wall makes them ideal for studies involving permeabilization.

In this report, we show (i) the intracellular copolymerization of ciliate and higher plant tubulins leading to hybrid MTs, (ii) the assembly of exogenous tubulin around the plant nucleus in interphase and telophase, and (iii) an intense incorporation of PA tubulin at the cell equator in the early stage of phragmoplast development. These results provide insight into the present debate on plant MTOC identification and on intracellular plant MT nucleation and elongation.

MATERIALS AND METHODS

Preparation of Tubulins and Antibodies. Tubulins were prepared from *Paramecium tetraurelia* (15) and from *Haemanthus* endosperm (21). Tubulin concentrations were determined according to Bradford (22), and purity was assessed by SDS/PAGE (23). Anti-PA-tubulin-specific antibodies (18, 19) were affinity-purified (15).

Cells. Living endosperm cells of *Haemanthus katherinae* Bak. (monocotyledons) were prepared as outlined (20).

Incorporation of PA Tubulin. *Haemanthus* cells were incubated in lysis buffer containing 65 mM Pipes, 25 mM Hepes, 33 mM potassium acetate, 5 mM MgCl₂, 10 mM EGTA, 0.5 mM EDTA, 1 μM pepstatin, 1 μM leupeptin, 10 μM dithiothreitol, 10 μM phenylmethylsulfonyl fluoride, 1 mM GTP, and saponin (200 μg/ml) (pH 6.94), adapted from Rozdzial and Haimo (24), and simultaneously supplemented with 1–5 μM PA tubulin for 3–10 min at 22°C. Cells were then briefly rinsed (10–20 s) in lysis buffer without PA tubulin, fixed 10 min in 1% glutaraldehyde in 0.1 M sodium phosphate (pH 6.9), and prepared for immunocytochemistry (25).

Immunocytochemistry. After preincubation in normal goat serum (diluted 1:20) in 10 mM Tris-buffered saline (pH 7.6), lysed cells were incubated in anti-PA-tubulin antibodies (0.5 μg/ml, 4 hr, 22°C) and then in fluorescein isothiocyanate-labeled goat anti-rabbit IgG (Nordic, Tilburg, The Netherlands) (diluted 1:20, 1 hr). For double-labeling, the preparations were incubated in a mixture of rabbit anti-PA-tubulin (0.5 μg/ml) with mouse monoclonal anti-β-neurotubulin (catalogue number 357, Amersham, Les Ulis, France; diluted 1:2000) and then incubated in a mixture of fluorescein isothiocyanate-conjugated goat anti-rabbit IgG (diluted 1:20) and rhodamine-conjugated sheep anti-mouse IgG (diluted 1:20). Observations were made by using a Leitz Orthoplan microscope with epifluorescence and a 63× NA 1.3 objective. Video images were recorded with a model WV 1850/G Newicon Panasonic camera and a model PVM 122 Sony

Abbreviations: MT, microtubule; MTOC, microtubule-organizing center; PA tubulin, *Paramecium* axonemal tubulin.

[†]Present address: Institut de Biologie Moléculaire des Plantes, Centre National de la Recherche Scientifique, 12 rue du Général Zimmer, 67084 Strasbourg Cedex, France.

[‡]To whom reprint requests should be sent at present address.

monitor connected to an image processor (Sapphire-Quantel, Montigny le Bretonneux, France) and photographed on the screen using a 36-mm Canon camera.

Electron Microscopy. Anti-PA-tubulin was revealed by 5-nm gold-labeled goat anti-rabbit IgG (Janssen Life Science Products, Beerse, Belgium) and processed for electron microscopy (25).

Immunoblot Analysis. After SDS/PAGE (7% polyacrylamide gels) and electrotransfer to nitrocellulose (26), the nitrocellulose blot was incubated overnight at 22°C with anti-PA-tubulin serum (diluted 1:300) or anti- β -neurotubulin (diluted 1:2000) in Tris-buffered saline. Detection was carried out with colloidal gold-conjugated antibodies, respectively, AuroProbe BLplus goat anti-rabbit IgG and goat anti-mouse IgG (diluted 1:100), followed by silver enhancement (AuroProbe BL plus and intenSE BL Kit, Janssen Life Science Products).

RESULTS

Specificity of Anti-PA-Tubulin Antibodies. By immunoblot analysis, we demonstrated that antibodies directed against PA tubulin (18, 19) did not react with higher plant tubulin (Fig. 1A). In contrast, anti-neurotubulin antibodies cross-reacted with plant and PA tubulins, although weaker with the latter (Fig. 1B). In *Haemanthus* cells, no fluorescence could be detected with anti-PA-tubulin antibodies, indicating the absence of reactivity with intracellular endosperm MTs (data not shown). Therefore, anti-PA-tubulin antibodies could be used to trace intracellular PA tubulin incorporation with high selectivity and anti-brain-tubulin monoclonal antibodies could be used to label the whole MT pattern.

Incorporation of PA Tubulin in Higher Plant Cells in Interphase. After a 5-min incubation with PA tubulin in lysis buffer and labeling with anti-PA-tubulin antibodies, *Haemanthus* endosperm cells exhibited a large population of short fluorescent MT segments ranging from 0.5 to 2 μ m, which were distributed throughout the cytoplasm (Fig. 2B and C). By means of double-label immunofluorescence, many of these MT segments were identified at the distal part of endogenous MTs that radiate from the nuclear envelope to the cell periphery (Fig. 2). The presence of copolymers composed of higher plant (unlabeled) and PA (labeled) tubulins was detected by electron microscopic immunogold-labeling and illustrated here in telophase (see Fig. 4). Optical sections through the nucleus revealed a dense population of short PA-tubulin-labeled MTs that emerged around the nuclear envelope, suggesting that their assembly occurred on the nuclear surface or in its close vicinity (Fig. 2C).

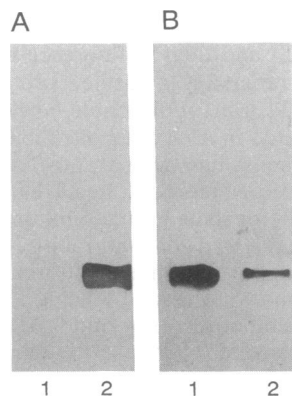


FIG. 1. Immunoblot analysis. PA (lanes 1) and *Haemanthus* (lanes 2) tubulins (5 μ g) were transferred and incubated with anti-PA-tubulin (A) or with anti- β -neurotubulin (B) antibodies. Note the entire lack of reactivity of anti-PA-tubulin against the plant tubulin (A) and the cross-reactivity between anti-neurotubulin antibodies and both tubulins (B).

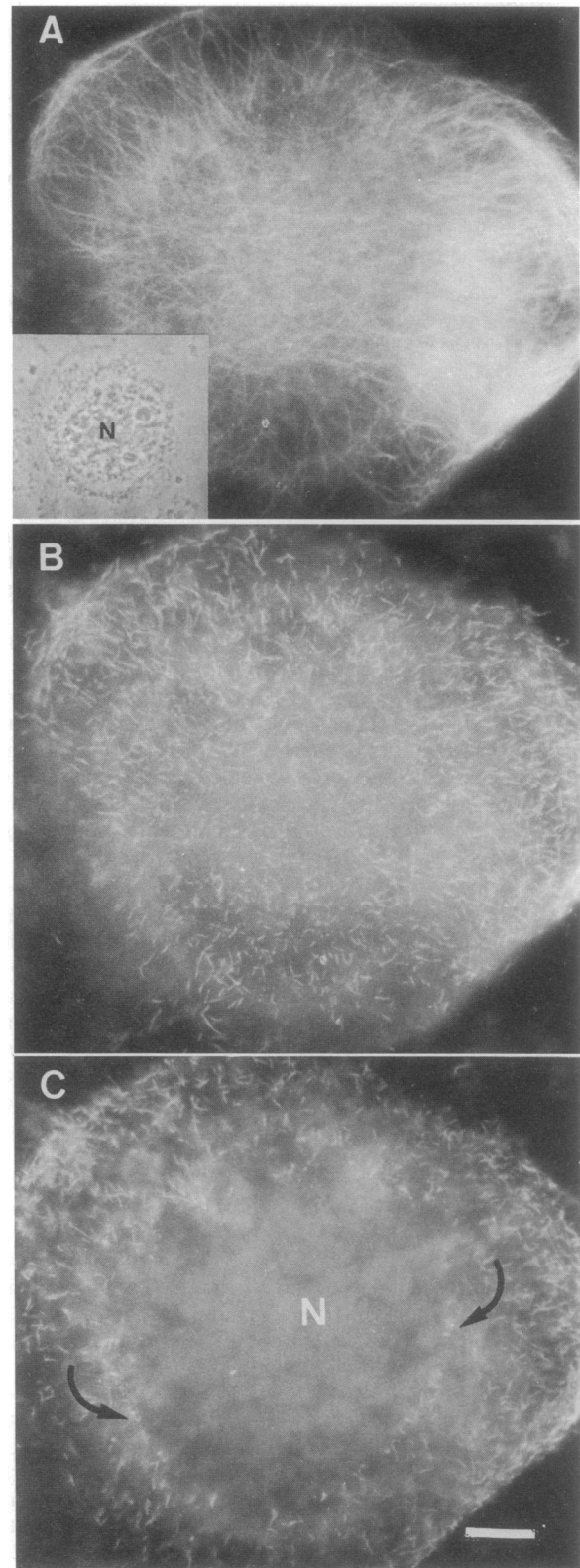


FIG. 2. Double-label immunofluorescence of a lysed endosperm cell in interphase incubated for 5 min in PA tubulin (4 μ M) before fixation. (A) Rhodamine anti- β -neurotubulin staining showing the whole intracellular MT network. (Inset) Phase-contrast micrograph of same cell. (B and C) Fluorescein isothiocyanate-conjugated anti-PA-tubulin staining of the cell in A showing MT segments distributed throughout the whole cytoplasm. (B) Tangential view of the nuclear surface. MT segments can be identified as the ends of endogenous MTs, indicating elongation. (C) Optical section through the nucleus. Short MT segments are distributed at the nuclear surface (curved arrows). N, nucleus. (Bar = 10 μ m.)

Mitosis. To study the origin of the plant phragmoplast, two stages were examined and compared: (i) late anaphase–early telophase transition, when the kinetochores reached the polar region and when the chromosome arms started to retract (Fig. 3 *A, B, and E*), and (ii) late telophase, when nuclei reformed and the cell plate began to develop at the equator (Fig. 3 *C, D, and F*). Cells were treated as above. In late anaphase, the interzone was occupied by thick bundles of MTs that elongated from the poles toward the equator (Fig. 3*A*), as demonstrated (6, 7). These MTs often intermingled at the equator (Fig. 3 *A and G*) where numerous vesicles accumulated (9, 10, 27). In such cells, incorporated PA tubulin appeared strikingly as a strong fluorescent ring at the equator (Fig. 3*B*), while short fluorescent MT segments were homogeneously dispersed within the whole endogenous MT population (Fig. 3 *B and H*). The intense equatorial fluorescence was mainly due to short labeled MT segments, mostly parallel to each other, and distributed within the region where endogenous interzonal MTs intermingled (Fig. 3 *A and B* and, for details, *G and H*). After anti-PA tubulin immunogold staining, these segments appeared to be labeled throughout their whole length (Fig. 4*A*). After double-label immunofluorescence staining, PA-tubulin-labeled segments within the interzone were identified as the ends of preexisting endogenous MTs, particularly those close to the edges of the cells (in Fig. 3, compare *A* with *B* and *C* with *D*). This was confirmed by electron microscopic observations (Fig. 4*B*).

Later, when telophase nuclei were being reconstructed and polar MTs were less abundant, the barrel-shaped phragmoplast was well developed with MTs 10–15 μm long on each side of the equator (Fig. 3 *C and F*). Most PA-tubulin-labeled segments were homogeneously dispersed within the phragmoplast (Fig. 3*D*) and could be identified at the ends of the developing phragmoplast MTs. However, an equatorial labeling with anti-PA-tubulin was also visible (Fig. 3*D*) although usually it seemed to be less intense than at the earlier stage (Fig. 3*B*). This sequence of events was followed in more than 40 cells. Electron microscopic observations confirmed that numerous fully PA-tubulin-labeled segments, such as those in Fig. 4*A*, were located at the equator, whereas short segments at the end of unlabeled (endogenous) MTs were detected at opposite sides of the equator within the phragmoplast. Around the daughter nuclei, PA tubulin incorporation was intense at the nuclear surface (Fig. 3*D*).

DISCUSSION

Herein we present a method for identifying the functional sites of MT assembly and potential MTOCs in the cells of a higher plant, *Haemanthus*. We developed a lysed model of endosperm cells in which the intracellular organization and the MT network were well preserved, as confirmed by electron microscopy (data not shown) and by comparison with reported immunostaining patterns (6–8). These lysed cells remained competent to assemble MTs (17) and to incorporate a foreign tubulin from *Paramecium* into hybrid polymers. These hybrid MTs were detected by a specific antibody (15, 18, 19) at sites inferred to be MTOCs and at the distal ends of plant MTs during interphase or mitosis through an elongation process. The situation is thus similar to that occurring after microinjection of PA (15) or labeled (13, 14) tubulins in metazoan cells. However, since no systematic study of the effects of tubulin concentration and other parameters on PA tubulin assembly was carried out, an analysis of the plant MT dynamics is precluded in the present *in vitro* model. Nevertheless, preliminary observations after microinjection of PA tubulin in living telophase *Haemanthus* cells showed, as in animal cells, an almost complete MT turnover within a few minutes (A. C. Schmit, personal communication).

The use of antibodies against pericentriolar material (3, 4) as well as studies of MT distribution and anchoring in *Haemanthus* cells (6–8, 12) strongly suggest that the plant nuclear surface may function as a nucleation site (for reviews, see refs. 28–30). Our data provide a functional evidence for tubulin assembly around the plant nucleus. The higher incorporation of perinuclear PA tubulin in prophase (data not shown) and in telophase relative to interphase also suggests that the MT nucleation capacity of the plant nuclear surface might be cell cycle-dependent.

There are two main hypotheses that may account for the origin of the phragmoplast–cell plate domain, which is a key element in the control of plant cytokinesis (for reviews, see refs. 28–30). Phragmoplast MTs could be (i) the remnants of half-spindle polar MTs that invaded the interzone in late anaphase or (ii) the result of new MT assembly at the equator during telophase.

According to the first hypothesis, phragmoplast MTs would arise from intermingling of spindle polar MTs which would progressively disassemble at their polar ends. The only nucleating centers would then be the mitotic poles in anaphase and the nuclear envelope of daughter nuclei in telophase. The major support of this hypothesis comes from (i) the polarity data (31) that indicated an equatorial zone of mixed polarities making a progressive transition between two MT populations of uniform and opposite polarities in each half-spindle (minus ends toward the poles and plus ends at the equator) and (ii) the lack of reactivity of the phragmoplast equatorial region toward antibodies against animal MTOCs (3, 32). In telophase, phragmoplast MT arrays that, for the most part, appear not to be connected to the poles (Fig. 3*C*) would arise from capping of the distal plus ends of polar MTs in dense material present at the equator (9, 10, 27) and then from disassembly at their minus ends. This would imply an unusual depolymerization direction, opposite to that observed in centriolar spindles. The occurrence of free minus ends, which display reduced dynamics (33), may account for the cold and drug resistance of these phragmoplast MTs (6, 34).

The intense incorporation of PA tubulin at the equator in late anaphase (Fig. 3 *A and B*) could be accounted for by elongation at the distal free plus ends of polar MTs that interdigitate. The pattern observed in telophase (Fig. 3 *C and D*) suggests, however, an elongation of phragmoplast MTs at the ends facing away from the equator. One should then admit that the MT ends that were postulated above to have depolymerized from the poles remain capable of accepting PA tubulin through elongation at minus ends.

In summary, this first hypothesis accounts well for MT polarity within the plant spindle, but it faces difficulties in explaining the origin of phragmoplast MTs and the incorporation pattern of exogenous tubulin in telophase described in this paper.

The second hypothesis assumes that the equatorial region of the phragmoplast functions as a MTOC and hence that phragmoplast MTs arise from new nucleation at the equator in telophase followed by elongation toward the daughter nuclei. Evidence in favor of this assumption is based upon (i) the restoration of phragmoplast birefringence after irradiation (35), (ii) the development of phragmoplast MTs independently of mitosis, as between nonsister nuclei during syncytium cellularization (6, 7, 9, 20), and (iii) the presence of MTOC-like (9, 10, 12, 27) MT-anchoring material in the cell-plate formation area.

The incorporation pattern of PA tubulin during successive stages of telophase, described here, provides evidence for this hypothesis. The intense equatorial labeling in early telophase, confirmed by electron microscopic observations of short fully gold-labeled MTs (Figs. 3*B* and 4*A*) and the distal MT labeling observed later in the barrel-shaped phrag-

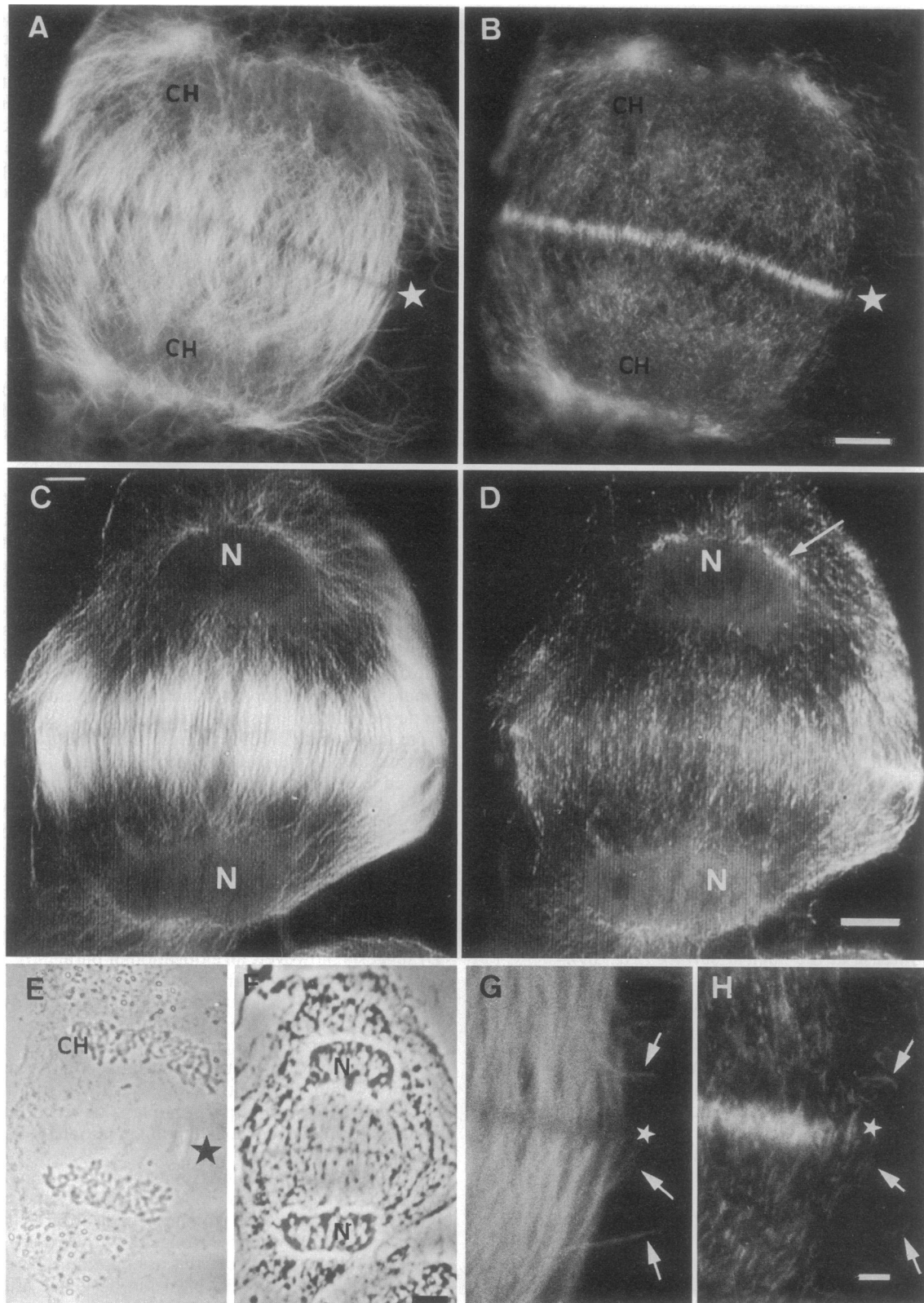


FIG. 3. Double-label immunofluorescence of two lysed endosperm cells incubated in PA tubulin ($4 \mu\text{M}$) during 5 min at two successive stages of telophase. (A, C, and G) Whole MT pattern revealed by rhodamine anti- β -neurotubulin staining. (B, D, and H) Fluorescein isothiocyanate-conjugated anti-PA-tubulin labeling. (E and F) The same cells in A and C, respectively, shown in phase-contrast. (A, B, and E) Early telophase. When chromosomes (CH) start to be decondensed, MT segments labeled with anti-PA-tubulin antibodies (B) are observed within the whole cell and correspond to the ends of polar MTs (compare A to B and, for details, G to H, arrows). An intense incorporation of PA tubulin is detected at the equator where short anti-PA-tubulin-labeled MT segments are superimposed to the overlapping region of endogenous MTs (star and for details see G and H). (C, D, and F) A later stage of telophase. (C) The nuclear envelope is reforming around the decondensed chromosomes and the barrel-shaped phragmoplast is developed. (D) Anti-PA-tubulin-labeled MT segments are dispersed within the phragmoplast while short segments are also detected at the equator. Intense PA tubulin assembly is seen around the daughter nuclei (long arrow). N, nucleus. (Bars: A–D, $10 \mu\text{m}$; G and H, $1 \mu\text{m}$.)

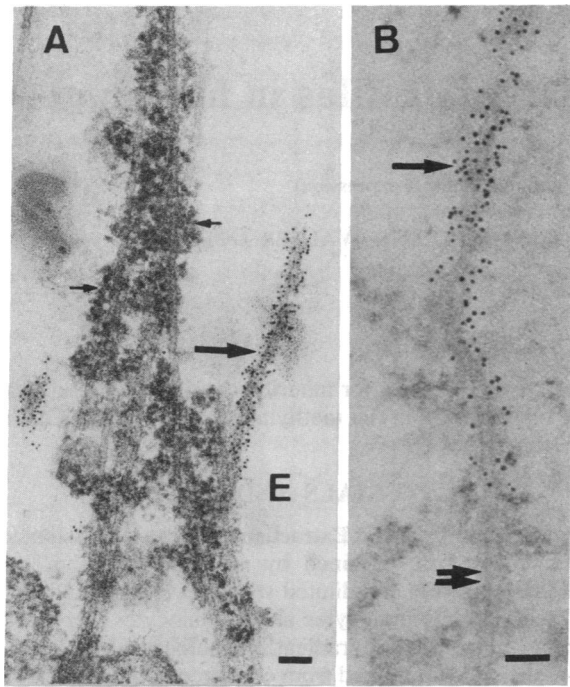


FIG. 4. Electron microscopy. Immunogold labeling of PA tubulin within the phragmoplast (same cell shown in Fig. 3 A and B). (A) Detail of the equatorial region. Endogenous unlabeled plant MTs intermingle and short MT segments (0.5–1 μm) that are intensely labeled with gold particles throughout their entire length are present (large arrow). Numerous ribosomes are present (small arrows). E, equator. (B) Detail of one hybrid MT indicating incorporation of PA tubulin (single arrow) at one end of the endogenous plant MT (unlabeled, double arrow). (Bars = 0.1 μm .)

moplast (Fig. 3D), are best accounted for by nucleation of MTs within the phragmoplast–cell plate area, followed by their distal elongation (up to 15 μm on average) toward the daughter nuclei. The new MTs may be codistributed with remnants of the overlapping polar MTs. If the equatorial MT nucleation in telophase occurred at the usual minus ends, it would generate phragmoplast MTs of polarity opposite to that of mitotic polar MTs. Hence, one may hypothesize also an unusual nucleation with phragmoplast MTs anchored by the plus ends at the MTOC. Tubulin assembly could then occur either at the anchored plus ends, which has not been observed for MTOCs and occurs only at kinetochores (14, 15), or, in an unusual way, at the distal minus ends. In the first case an exclusive equatorial labeling of PA tubulin would be expected in the phragmoplast in contrast to our observations, whereas under the second assumption the predicted incorporation pattern agrees with that actually obtained.

Therefore, the PA tubulin incorporation pattern that we observed during anaphase–telophase fits the best with our favored model in which the equatorial region of the phragmoplast acts as a MTOC. Thus, with observations of actin dynamics *in vivo* in telophase (36), our data suggest that selective cytoskeleton assembly properties are associated with this strategic site of new cell membrane and cell wall assembly.

In conclusion, polymerization of exogenous *Paramecium* tubulin into lysed *Haemaphysalis* cells provides insight, based on a functional assay, into current and debated hypotheses on the MT nucleation capacity of the plant nuclear envelope and the phragmoplast equator.

We thank Mrs. Monique Wehr for her assistance in preparing the manuscript. We thank U. Sorhannus for revising this manuscript and H. Le Guyader for numerous fruitful discussions. This work was supported by the Centre National de la Recherche Scientifique and the Ministère de la Recherche et de l'Enseignement Supérieur (87T0233).

1. Calarco-Gillam, P. D., Siebert, M. C., Hubble, R., Mitchison, T. & Kirschner, M. (1983) *Cell* **35**, 621–629.
2. Mitchison, T. & Kirschner, M. (1984) *Nature (London)* **312**, 232–237.
3. Clayton, L. C., Black, C. M. & Lloyd, C. W. (1985) *J. Cell Biol.* **101**, 319–324.
4. Wick, S. M. (1985) *Cytobios* **43**, 285–294.
5. Harper, J. D. I., Mitchison, J. M., Williamson, R. E. & John, P. C. L. (1989) *Cell Biol. Int. Rep.* **13**, 471–483.
6. Bajer, A. S. & Molè-Bajer, J. (1982) in *Organisation of the Cytoplasm*, Cold Spring Harbor Symposia (Cold Spring Harbor Lab., Cold Spring Harbor, NY), Vol. 46, pp. 263–283.
7. De Mey, J., Lambert, A. M., Bajer, A. S., Moeremans, M. & De Brabander, M. (1982) *Proc. Natl. Acad. Sci. USA* **79**, 1898–1902.
8. Schmit, A. C., Vantard, M., De Mey, J. & Lambert, A. M. (1983) *Plant Cell Rep.* **2**, 285–288.
9. Bajer, A. S. (1968) *Chromosoma* **24**, 383–417.
10. Hepler, P. K. & Jackson, W. T. (1968) *J. Cell Biol.* **38**, 437–446.
11. Pickett-Heaps, J. D. (1969) *Cytobios* **43**, 285–294.
12. Lambert, A. M. (1980) *Chromosoma* **76**, 295–308.
13. Soltys, B. J. & Borisy, G. G. (1985) *J. Cell Biol.* **100**, 1682–1689.
14. Mitchison, T., Evans, L., Schulze, E. & Kirschner, M. (1986) *Cell* **45**, 515–527.
15. Geuens, G., Hill, A. M., Levilliers, N., Adoutte, A. & De Brabander, M. (1989) *J. Cell Biol.* **108**, 939–953.
16. Prescott, A. R., Foster, K. E., Warn, R. M. & Gull, K. (1989) *J. Cell Sci.* **92**, 595–605.
17. Vantard, M. & Lambert, A. M. (1988) in *Structure and Functions of the Cytoskeleton: Biological and Physiopathological Aspects*, ed. Rousset, B. (Libbey, Paris), Vol. 171, p. 551.
18. Cohen, J., Adoutte, A., Grandchamp, S., Houdebine, L.-M. & Beisson, J. (1982) *Biol. Cell* **44**, 35–44.
19. Adoutte, A., Claisse, M., Maunoury, R. & Beisson, J. (1985) *J. Mol. Evol.* **22**, 220–229.
20. Bajer, A. S. & Molè-Bajer, J. (1986) *J. Cell Biol.* **102**, 263–281.
21. Picquot, P. & Lambert, A. M. (1988) *J. Plant Physiol.* **132**, 561–568.
22. Bradford, M. M. (1976) *Anal. Biochem.* **72**, 248–254.
23. Laemmli, U. K. (1970) *Nature (London)* **227**, 680–685.
24. Rozdzial, M. M. & Haimo, L. T. (1986) *J. Cell Biol.* **103**, 2755–2764.
25. Vantard, M., Lambert, A. M., De Mey, J., Picquot, P. & Van Eldik, L. J. (1985) *J. Cell Biol.* **101**, 488–499.
26. Towbin, H., Staehelin, T. & Gordon, J. (1979) *Proc. Natl. Acad. Sci. USA* **76**, 4350–4354.
27. Lambert, A. M. & Bajer, A. S. (1972) *Chromosoma* **39**, 101–144.
28. Hepler, P. K. & Wolniak, S. M. (1984) *Int. Rev. Cytol.* **90**, 169–238.
29. Seagull, R. W. (1989) *Crit. Rev. Plant Sci.* **8**, 131–167.
30. Baskin, T. I. & Cande, W. Z. (1990) *Annu. Rev. Plant Physiol. Plant Mol. Biol.* **41**, 277–315.
31. Euteneuer, U., Jackson, W. T. & McIntosh, J. R. (1982) *J. Cell Biol.* **94**, 644–653.
32. Wick, S. M. (1985) *Cell Biol. Int. Rep.* **9**, 357–371.
33. Walker, R. A., O'Brien, E. T., Pryer, N. K., Soboeiro, M. F., Voter, W. A., Erickson, H. P. & Salmon, E. D. (1988) *J. Cell Biol.* **107**, 1437–1448.
34. Schmit, A. C. & Lambert, A. M. (1988) *Biol. Cell* **64**, 309–319.
35. Inoué, S. (1964) in *Primitive Motile Systems in Cell Biology*, eds. Allen, R. D. & Kamiya, N. (Academic, New York), pp. 549–598.
36. Schmit, A. C. & Lambert, A. M. (1990) *The Plant Cell* **2**, 129–138.